Available online at www.sciencedirect.com

SCIENCE DIRECT®

Journal of Luminescence 119–120 (2006) 242–247

JOURNAL OF LUMINESCENCE

www.elsevier.com/locate/jlumin

Temperature-enhanced ultraviolet emission in ZnO thin film

Y.J. Zhang[a], C.S. Xu[a,*], Y.C. Liu[a], Y.X. Liu[a], G.R. Wang[a], X.W. Fan[b]

[a]*Center for Advanced Opto-Electronic Functional Material Research, Northeast Normal University, Changchun 130024, People's Republic of China*

[b]*Key Laboratory of Excited State Processes, Changchun Institute of Optics, Fine Mechanics and Physics, Chinese Academy of Sciences, 16-Dongnanhu Avenue, Changchun 130033, People's Republic of China*

Abstract

We have studied the structural and optical properties of ZnO thin films prepared by thermal oxidation of ZnS films deposited by plasma assisted electron-beam evaporation on Si(1 0 0) substrates. The transformation from zinc blende ZnS to hexagonal wurtzite ZnO is confirmed by Raman and X-ray diffraction (XRD) measurement. For the sample thermally oxidized at 600 °C for 2 h, a novel UV emission peak I_x located at 3.22 eV (385 nm) has been observed. The temperature-dependent photoluminescence spectra show that the integrated intensity of I_x increases exponentially with increasing temperatures within the measuring temperature range, from 80 to 300 K, but the peak position remains nearly constant. We explain this behavior in terms of electron tunneling into the radiative recombination centers.

Keywords: ZnO; PL; Temperature-dependent photoluminescence; II–IV semiconductors; Thermal oxidation

---

1. Introduction

The wide band gap semiconductor ZnO, with a room-temperature (RT) band gap of 3.37 eV and an exciton binding energy of 60 meV, has attracted much attention because of its promising applications in RT excitonic UV optoelectronic devices [1]. Generally, the photoluminescence (PL) of ZnO may be roughly classified into two groups as due to free-exciton (FE) and bound-exciton (BE) emissions in the UV region and deep level emissions in the visible region [2–4]. But despite the extensive studies, there are still some fundamental properties of the PL of ZnO which are not fully understood. One of such issues is the temperature dependence of the integral intensity and position of some of the UV emission peaks. Most researchers have found that when temperature increases, affected by the thermal quenching processes and the shrinkage of the band gap energy, the UV emission peaks weaken and move to lower energy side. But Zhang et al. [5] have reported an UV emission peak located at 290 nm, its integral intensity increases with temperature from 7 to 119 K; Zhao et al. [6] have reported an

---

*Corresponding author. Tel./fax: + 86 431 5098803.
E-mail address: csxu@nenu.edu.cn (C.S. Xu).

0022-2313/$ - see front matter © 2006 Published by Elsevier B.V.
doi:10.1016/j.jlumin.2005.12.037

UV emission peak, its position remains nearly unchanged with increasing temperature.

In this work, the structural and optical properties of thin ZnO films prepared by thermal oxidation of ZnS films were investigated by using resonance Raman, X-ray deflection (XRD) and temperature-dependent PL spectroscopy. For the sample thermally oxidized at 600 °C for 2 h, an unidentified UV emission peak located at 3.22 eV (385 nm) was detected. The integral intensity of this emission peak increased exponentially with increasing temperatures from 80 to 300 K, but the peak position remained nearly constant.

2. Experiments

ZnO thin films were prepared through low-temperature thermal oxidation of ZnS film deposited on Si(1 0 0) substrate using an O:Ar (1:1) plasma assisted electron-beam evaporation method. The Si substrate was cleaned by standard RCA process and was bombarded by Ar plasma for 10 min to remove the oxide layer before deposition. The base pressure of the growth chamber was 2.0×10^{-3} Pa and the working pressure was controlled at 1.1×10^{-2} Pa. The temperature of the substrate was kept at 210 °C during the deposition process. The beam current of the electron was 12 mA and the beam voltage was 6.5 kV. After 15 min deposition, the sample was cut into pieces and four pairs of such pieces were thermally oxidized in the O_2 ambient at 400, 500, 600 and 700 °C for 2 h, respectively. To slow down the speed of the transformation from ZnS to ZnO so as to investigate the oxidation process more efficiently, we put each pair of pieces face to face during the oxidization process.

The structural and optical properties of the as-grown and oxidized samples were characterized with XRD, resonance Raman spectroscopy and temperature-dependent PL spectroscopy. The XRD spectra were collected on a D/max-RA X-ray diffractometer (Rigaku) with Cu Kα line of 0.154 nm. Micro-Raman and PL measurements were conducted with a J-Y UV-lamb micro-Raman spectrometer using a He–Cd laser (325 nm) as an excitation light source.

3. Results and discussions

3.1. Structure

Fig. 1 shows the typical resonance Raman spectra of the as-deposited ZnS film and the films oxidized at 400, 500, 600 and 700 °C for 2 h, respectively. Under the O:Ar (1:1) plasma assistant, some ZnO nanocrystals were formed and embedded in the ZnS film during the deposition process. As a result, in the resonance Raman spectrum of the as-grown film, apart from the strong longitudinal optical (LO) multiphonon lines of ZnS [7], we can also see the 1LO and 2LO phonon lines of hexagonal wurtzite ZnO [8]. These ZnO nanocrystals, serving as nucleation cores, make the transformation from ZnS to ZnO more readily.

After the samples were oxidized at elevated temperatures, the intensity of the ZnS LO phonon lines decreased. At the same time, the intensity of the ZnO LO phonon lines increased. This indicates that the ZnO cores grew in size and the ZnS was transformed into ZnO gradually. For the sample oxidized at 600 and 700 °C, the Raman signals of ZnS disappeared, only the Raman signals of ZnO was detected. The ZnS was transformed into ZnO completely. The inset in Fig. 1 is the XRD patterns

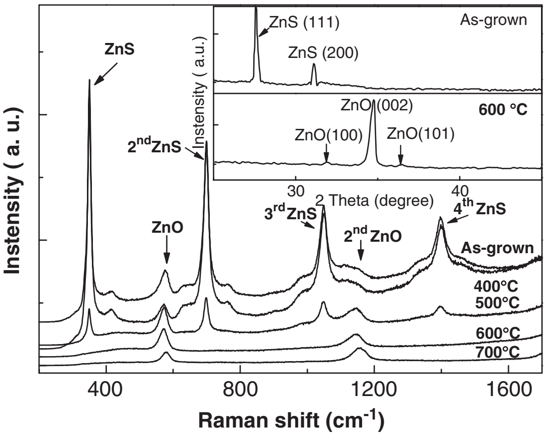

Fig. 1. Resonance Raman spectra of the as-grown ZnS film and the films oxidized at different temperatures for 2 h. Inset is the XRD spectra of the as-grown ZnS film and the film oxidized at 600 °C for 2 h.

of the as-grown ZnS film and the film oxidized at 600 °C. The as-grown film shows two diffraction peaks at 28.84° and 33.54°, which correspond to the (1 1 1) and (2 0 0) diffraction of the zinc blende ZnS. It is interesting to note that although the existence of the ZnO nanocrystals formed in the deposition process has been confirmed by the Raman scattering measurement, no XRD signal from ZnO was detected. This means that Raman scattering is more sensitive than X-ray diffraction to traces of nanocrystals. For the film oxidized at 600 °C, there are three diffraction peaks at 31.8°, 34.74° and 36.47°, which correspond to the (1 0 0), (0 0 2) and (1 0 1) diffraction from wurtzite ZnO, no diffraction peak from ZnS was detected. These results together with the Raman scattering results described above confirm that when oxidized at 600 °C or higher temperatures the ZnS thin films transformed into ZnO films completely.

3.2. Photoluminescence

Fig. 2 is the RT PL spectrum of the sample oxidized at 600 °C, in which the resonance Raman data show that only ZnO phase is present. The most prominent emission band located at 3.22 eV (385 nm) is signified as I_x. The line shape of I_x is broad and asymmetric.

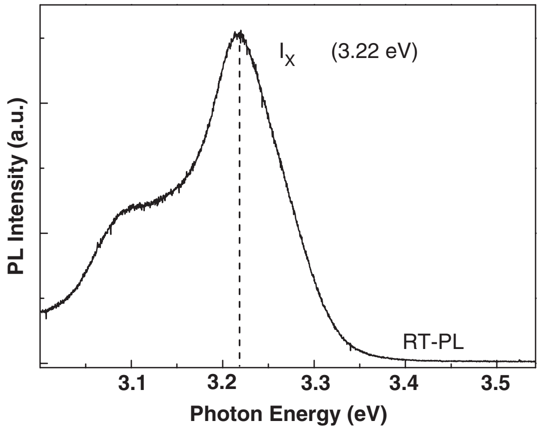

Fig. 2. The room-temperature PL spectrum of the film oxidized at 600 °C for 2 h.

To further investigate the properties of this UV emission peak I_x, the temperature-dependent PL spectra were recorded (Fig. 3). The PL spectrum at 80 K is dominated by the normal excitonic UV emission band [9]. The FE peak and its phonon replica (FE-LO) and the shallow BE peak can be resolved by Gaussian fitting. The temperature dependence of the integrated PL intensity of the FE peak is shown in Fig. 4(a). The experimental data have been fitted with the thermal quenching equation [10]:

$$I(T) = I_0/[1 + A\exp(-E/k_BT)],$$

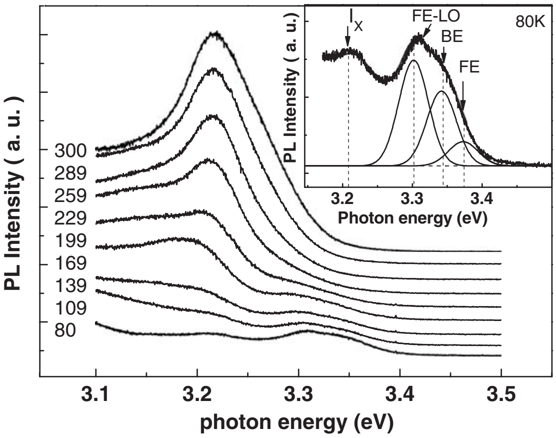

Fig. 3. Temperature dependence of the PL spectra of the thin film oxidized at 600 °C for 2 h in the temperature range of 80–300 K. The inset figure is the PL spectrum at 80 K.

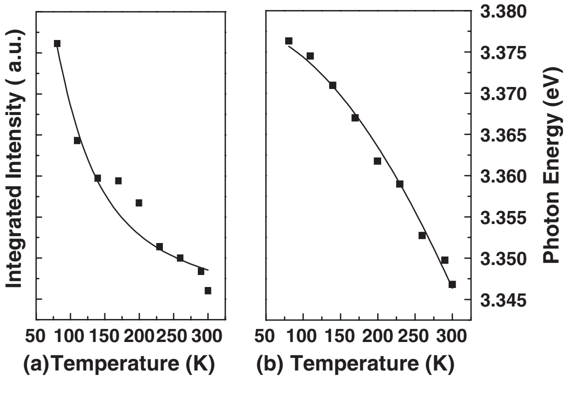

Fig. 4. (a) The integrated PL intensity of the free exciton peak as a function of temperature ranging from 80 to 300 K. The solid line is the theoretical fit to the experimental data using $I(T) = I_0/[1 + A\exp(-E/k_BT)]$. (b) The peak energy of the free exciton as a function of temperature ranging from 80 to 300 K. The solid line is the theoretical fit to the experimental data using $E(T) = E_0 - \alpha T^2/(T + \beta)$.

where E is the thermal activation energy, I_0 is the PL intensity at $T = 0$ K, and k_B is the Boltzmann constant. The best fit has been obtained for $E = 59.9$ meV, which is consistent with the exciton binding energy (59 meV) in bulk ZnO [11]. Fig. 4(b) shows the peak position of FE at different temperatures from 80 to 300 K. It can be seen that the peak shifted to lower energies with increasing temperature due to the shrinkage of the band gap energy with increasing temperature. Assuming that the exciton binding energy does not change with temperature, the temperature dependence of the free excitonic band gap of ZnO can be well approximated by the empiric Varshni formula [12]:

$$E(T) = E(0) - \alpha T^2/(T + \beta),$$

where $E(0)$ is the excitonic band gap energy of ZnO at 0 K, α, β are the Varshni's coefficients. By fitting the Varshni formula to the experimental data, $E(0) = 3.38$ eV, $\alpha = 9.00 \times 10^{-4}$ eV/K, and $\beta = 2.23 \times 10^3$ K has been obtained, these values are in reasonable agreement with those reported in literatures for bulk and epitaxial thin films [13–15]. As temperature increases, the bound excitonic feature gets weakened and finally disappears due to the thermal ionization of the BE.

The temperature dependence of peak I_x exhibits a completely different behavior compared to that of the FE peak. The emission intensity of I_x is strengthened with increasing temperature and its peak position remains nearly constant (Fig. 5). Similar phenomena have been reported before, but only at very low temperatures and within very narrow temperature ranges (as shown in Table 1). In our study, as shown in Fig. 5, the PL intensity of I_x increased with increasing temperature within the whole measurement temperature range, i.e. from 80 K all the way through to 300 K, and no evidence of saturation was observed even up to 300 K. At RT, I_x became the dominant feature in the PL spectrum. The full-width at half-maximum (FWHM) of I_x is much broader than that of the FE emission peak. Table 1 also shows reports of peaks with similar energy to I_x, they are attributed to various mechanisms and their peak position all tend to shift with changing temperatures. There are also reports about some unconventional UV emissions from ZnO which are not originated from the emission of excitonic transitions [20–22], but no temperature enhancement was observed.

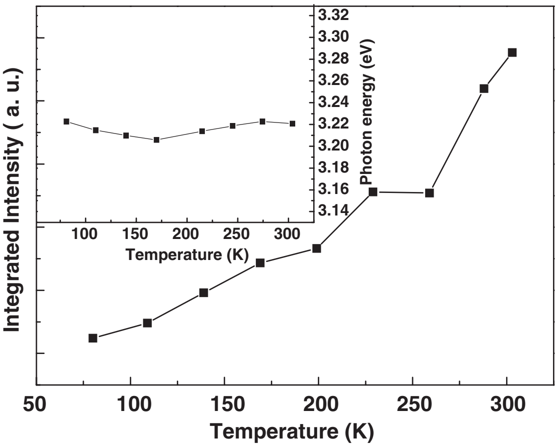

Fig. 5. The integrated intensity of the peak I_x as a function of temperature ranging from 80 to 300 K. The inset is temperature dependence of the peak position of I_x.

Careful fitting to the experimental data shows that the intensity of I_x increases exponentially with increasing temperature, i.e. the integrated intensity of I_x is proportional to $\exp(T/T_0)$ and best fit can be obtained for $T_0 = 117$ K. This is qualitatively different from the thermal activation law, where the intensity increases proportional to $\exp(T_0/T)$. Actually, it has long been observed that the temperature dependence of the intensity of PL in amorphous semiconductors obey the $\exp(-T/T_0)$ law [23]. Street et al. [24] suggested that this kind of temperature dependence is related to the tunneling away of electron from the radiative recombination site to a trap. Assuming that there is a spatially varying band gap and that the band minima are parabolic, the calculations carried out by Street et al. shows that the nonradiative transition probability is proportional to $\exp(T/T_0)$ and results in a PL decrease proportional to $\exp(-T/T_0)$.

In our case, because the samples were obtained through thermal oxidation of ZnS at relatively low temperatures which would encourage imperfect crystal growth, we propose that band gap fluctuations may occur in the ZnO film, especially in the vicinity of the grain boundary regions. And some

Table 1
Reported peaks with similar energy position with I_x and reported results in which temperature enhancement occurs

Author	Energy (eV)	Assignment	PL enhancement region
Hamby et al. and Teke et al. [15,16]	3.223	Second LO phonon replica of A-free exciton	
Teke et al. [16]	3.2176	Bond to bond transition (donor to acceptor)	
Hamby et al. [17]	3.2018	Donor–acceptor pair transition	
Thonke et al. [18]	3.236	Free electron–acceptor transition	30–120 K
Xiong et al. [19]	3.199	Two phonon replica of neutral donor bond exciton complex	16–62 K
Hamby et al. [15]	3.364	Neutral donor bond exciton emission	6.4–60 K
Zhang et al. [5]	3.262	Near band edge emission	7–119 K

defects or unintentionally doped impurities may act as the trap. The main difference here is that the traps are centers of radiative recombination. After the tunneling of the electron into the trap, a radiative recombination takes place, thus leads to a PL with its intensity rising proportional to $\exp(T/T_0)$. Luerben et al. [25] have already modeled the local recombination in type-II GaAs/AlAs superlattices in terms of the electron tunneling into the luminescing states.

4. Conclusions

In conclusion, we have investigated the structural and optical properties of ZnO thin films prepared by thermal oxidation of ZnS films deposited by plasma assisted electron-beam evaporation on Si(1 0 0) substrates. For the sample thermally oxidized at 600 °C for 2 h, a novel UV emission peak I_x located at 3.22 eV (385 nm) has been observed. The temperature-dependent PL spectra show that the integrated intensity of I_x rises proportional to $\exp(T/T_0)$ within the measuring temperature range, from 80 to 300 K, but the peak position of I_x remains nearly constant. We attribute this behavior to the electron tunneling into the radiative recombination center.

Acknowledgments

This work is supported by Cultivation of the Key Scientific and Technical Innovation Project (No. 704017), Ministry of Education of China; National Natural Science Foundation of China (No. 60376009, 60278031) and Science Foundation for Young Teachers of Northeast Normal University (No. 20050207).

References

[1] U. Ozgur, Ya. I. Alivov, C. Liu, A. Teke, M.A. Reschikov, S. Dogan, V. Avrutin, S.J. Cho, H. Morkoc, J. Appl. Phys. 98 (2005) 041301.
[2] R. Dingle, Phys. Rev. Lett. 23 (1969) 579.
[3] K. Vanheusden, C.H. Seager, W.L. Warren, D.R. Tallant, J.A. Voigt, Appl. Phys. Lett. 68 (1996) 403.
[4] M. Anpo, Y. Kubokawa, J. Phys. Chem. 88 (1984) 5556.
[5] G.B. Zhang, C.S. Shi, Z.F. Han, J.Y. Shi, Z.X. Fu, M. Kirm, G. Zimmerer, Chin. Phys. Lett. 18 (2001) 441.
[6] Q.X. Zhao, M. Willander, R.E. Morjan, Q.H. Hu, E.E.B. Campbell, Appl. Phys. Lett. 83 (2003) 165.
[7] J. Serrano, A. Cantarero, M. Cardona, N. Garro, R. Lauck, R.E. Tallman, T.M. Ritter, B.A. Weinstein, Phys. Rev. B 69 (2004) 014301.
[8] T.C. Damen, S.P. Porto, B. Tell, Phys. Rev. 142 (1966) 570.
[9] J.G. Ma, Y.C. Liu, C.S. Xu, Y.X. Liu, C.L. Shao, H.Y. Xu, J.Y. Zhang, Y.M. Lu, D.Z. Shen, X.W. Fan, J. Appl. Phys. 97 (2005) 103509.
[10] T. Makino, K. Tamura, C.H. Chia, Y. Segawa, M. Kawasaki, A. Ohtomo, H. Koinuma, J. Appl. Phys. 93 (2003) 5929.
[11] U. Koch, A. Fojtik, H. Weller, A. Henglein, Chem. Phys. Lett. 122 (1985) 507.
[12] Y.P. Varshni, Physica 34 (1967) 149.
[13] R.H. Callender, S.S. Sussman, M. Selders, R.K. Chang, Phys. Rev. B 7 (1973) 3788.
[14] C. Klingshrin, Phys. Stat. Sol. (B) 71 (1975) 547.
[15] D.W. Hamby, D.A. Lucca, M.J. Klopfstein, G. Cantwell, J. Appl. Phys. 93 (2003) 3214.

[16] A. Teke, U. Ozgur, S. Gudan, X. Gu, H. Morkoc, B. Nemeth, J. Nause, H.O. Everitt, Phys. Rev. B 70 (2004) 195207.

[17] D.W. Hamby, D.A. Lucca, M.J. Klopfstein, J. Appl. Phys. 97 (2005) 043504.

[18] K. Thonke, T. Grube, N. Teofilov, R. Schonfelder, A. Waag, R. Sauer, Physica B 308 (2001) 945.

[19] G. Xiong, K.B. Ucer, R.T. Williams, J. Lee, D. Bhattacharyya, J. Metson, P. Evans, J. Appl. Phys. 97 (2005) 043528.

[20] V.A. Fonoberov, A.A. Balandin, Appl. Phys. Lett. 85 (2004) 5971.

[21] C.L. Yang, J.N. Wang, W.K. Ge, L. Guo, S.H. Yang, D.Z. Shen, J. Appl. Phys. 90 (2001) 4489.

[22] Q.X. Zhao, M. Willander, R.E. Morjan, Q.H. Hu, E.E.B. Campbell, Appl. Phys. Lett. 83 (2003) 165.

[23] D. Kaplan, N. Sol, G. Velasco, P.A. Thomas, Appl. Phys. Lett. 33 (1978) 440.

[24] R.A. Street, T.M. Searle, I.G. Austin, Philos. Mag. 30 (1974) 1181.

[25] D. Luerben, A. Oehler, R. Bleher, H. Kalt, Phys. Rev. B 59 (1999) 15862.